Physics – Uspekhi **58** (5) 486 – 494 (2015)

CONFERENCES AND SYMPOSIA

PACS numbers: 29.40.Ka, 95.55.Vj, 96.50.S –

110th ANNIVERSARY OF THE BIRTH OF P A CHERENKOV

Cherenkov water detector NEVOD

A A Petrukhin

DOI: 10.3367/UFNe.0185.201505i.0521

Contents

Abstract. A unique multipurpose Cherenkov water detector, the NEVOD facility, uses quasispherical measuring modules to explore all the basic components of cosmic rays on Earth's surface, including neutrinos. Currently, the experimental complex includes the Cherenkov water detector, a calibration telescope system, and a coordinate detector. This paper traces the basic development stages of NEVOD, examines research directions, presents the results obtained, including the search for the solution to the 'muon puzzle', and discusses possible future development prospects.

Keywords: Cherenkov radiation, Cherenkov detectors, photomultipliers, cosmic rays, muons, cascade showers, extensive air showers

1. Introduction

Cherenkov water detectors (CWDs) represent the most large-scale example of the application of Cherenkov radiation for implementing fundamental and applied investigations. The scales of modern CWDs amount to kilotonnes (Super-Kamiokande [1]), megatonnes (Baikal [2], ANTARES (Astronomy with a Neutrino Telescope and Abyss environmental RESearch) [3]), and gigatonnes (IceCube [4]). And although water is not the best substance for creating nuclear-physics facilities (low density and small atomic numbers of elements involved, nearly equal the radiation and nuclear lengths), certain of its parameters (good transparency, low cost, and possibility of using natural water volumes) render it practically the only substance for creating detectors with masses of several dozen or hundred megatonnes or more.

The epoch of violent CWD development started in the 1970s, when detectors were requested for studies of neutrinos of TeV energies: first, in searches for the W-boson and estimating its mass, and then, when the W-boson was discovered in collider experiments, in searches for extraterrestrial sources of such neutrinos. Calculations of the expected counting rate of events with interactions of TeV neutrinos demonstrated that, to obtain reasonable statistics, the creation of a detector with a mass of several hundred megatonnes was required (DUMAND project — Deep Underwater Muon And Neutrino Detector [5]).

The next problem, the solution of which required CWDs, was the search for proton decay. Estimates of the expected number of decays showed that detectors with a mass on the order of 1 kt were needed. Although detectors with such masses could be (and had been) constructed utilizing other, heavier, materials (NUSEX (NUcleon Stability EXperiment) [6], Frejus [7]), water detectors had an important advantage — practically the same registration probability of proton decay at any point of the detector. Two such detectors were created: Kamiokande, 3 kt in mass [8], and IMB (Irvine — Michigan — Brookhaven), 8 kt in mass [9].

2. Types of Cherenkov water detectors

The main detecting element that registers the Cherenkov radiation of charged particles is composed of photomultiplier tubes (PMTs). Their spatial arrangement permits distinguishing between peripheral and volume (lattice)

A A Petrukhin National Research Nuclear University MEPhI (Moscow Engineering Physics Institute), Kashirskoe shosse 31, 115409 Moscow, Russian Federation
E-mail: AAPetrukhin@mephi.ru

Received 23 March 2015
Uspekhi Fizicheskikh Nauk **185** (5) 521 – 530 (2015)
DOI: 10.3367/UFNr.0185.201505i.0521
Translated by G Pontecorvo; edited by A Radzig

CWDs. PMTs in peripheral detectors are positioned along the inner walls of the water reservoir and provide a 4π-geometry for the registration of Cherenkov radiation of charged particles arriving from all directions. This circumstance was important for the search for proton decays whose products could propagate in any direction. An essential disadvantage of peripheral detectors lies in the restriction imposed on their size, determined by the absorption length of Cherenkov radiation in water. If the detector dimensions exceed the absorption length, zones of reduced registration probability start to appear, and then dead zones also originate.

The detectors created for searches for proton decay [8, 9] were of the peripheral type, since their dimensions [$(15-20)^3$ m^3] were inferior to the absorption length of Cherenkov radiation in highly purified water.

In the case of neutrino detectors, lattice structures are more convenient, since it is possible to construct detectors of any dimension by a simple increase of the number of strings holding the PMTs. The distances between photomultipliers in a string and between the very strings are determined by the absorption length of Cherenkov radiation, while the number of strings has no limit of a fundamental character. In neutrino detectors, the 4π-geometry is not important either, since registration is mostly performed of the particle flux from the lower hemisphere, owing to the very large background of other particles (mainly muons) arriving from the upper hemisphere. At the same time, registration of particles from the upper hemisphere and respective investigations are of interest on their own.

The idea of constructing a multipurpose CWD deployed on the surface of Earth for carrying out studies of all the main cosmic ray components was first put forward in 1977 at a Conference in Vladivostok, where the participation of Soviet scientists in realizing the DUMAND project and the construction of a Soviet installation of such a class were discussed. The Cherenkov water detector NEVOD was conceived, first, as a laboratory prototype of future installations like DUMAND, second, as a neutrino water detector (hence the abbreviation NEVOD [10]: Russian 'voda' means water) with a very high ($\sim 10^{10}$) rejection level of background events, and third, as a detector of other cosmic ray (CR) components, including muons (single and in bundles), and of extensive air showers (EASs). This approach turned out to be fruitful and, subsequently, the Milagro detector [11] was constructed for investigating fluxes of high-energy gamma quanta by distinguishing between EASs due to γ-quanta and those due to charged particles of the primary cosmic radiation (PCR) by the muon component registered with the aid of CWDs. An attempt was also made to deploy a large-scale neutrino detector on Earth's surface (NET (Neutrino Telescope) project [12]), which, however, was not realized.

In accordance with the formulated tasks, NEVOD was to have a volume structure (as a prototype of larger scale detectors) and at the same time to serve as a 4π-detector (for the registration of particles arriving from the upper hemisphere). For this purpose, use was required either of photomultiplier tubes with spherical photocathodes or of some combination of PMTs with flat photocathodes providing an isotropic response to Cherenkov radiation.

3. Quasispherical modules

Most photomultiplier tubes produced industrially — and in the 1970s practically all — have flat photocathodes. When the registered Cherenkov radiation arrives from a certain direction, the response of such PMTs depends on the angle of incidence of the radiation upon the photocathode plane and, consequently, on the angle between the registered charged particle trajectory and the photomultiplier axis. If one takes into account that the PMT response also depends on the distance to the charged particle track, significant uncertainties arise in the interpretation of measurement results. Indeed, the photomultiplier response can be written in the first approximation as

$$N(R,\alpha) = N_0 \frac{S\cos\alpha}{R} \exp\left(-\frac{R}{L}\right), \quad (1)$$

where N_0 is the number of Cherenkov photons emitted from a unit length of the charged particle track, S is the photocathode area, R is the distance between the track and the photocathode, α is the angle of incidence of the Cherenkov radiation on the photocathode, and L is the absorption length of Cherenkov photons, averaged over their frequency spectrum.

For elimination of the indicated drawback, photomultipliers were developed with hemispherical photocathodes whose response did not depend on the angle of incidence of the Cherenkov radiation (naturally, within certain limits). Such photomultipliers find application in the Baikal [2] and IceCube [4] experiments, the main purpose of which consists in registering neutrino events from the lower hemisphere. At the same time, such PMTs pointing in the same direction do not provide good conditions for registration of the CR muon component arriving from the upper hemisphere.

For CWDs deployed on Earth's surface, the necessity of registering particles arriving along directions not only from above and from below, but also close to the horizon is relevant. Therefore, a module comprising several PMTs was constructed, which was termed a quasispherical module (QSM). There are several possible structures consisting of photomultipliers with flat photocathodes, the total response of which is independent of the arrival direction of Cherenkov radiation. Such a property is exhibited by structures in which photomultipliers are positioned at the centers of the faces and/or on the truncated vertices of proper polyhedrons. In the case of R values exceeding the module dimensions, their response

$$A(R) = \sqrt{\sum_{i=1}^{n}\left(\frac{N_0 S}{R}\exp\left(-\frac{R}{L}\right)\cos\alpha_i\right)^2} \quad (2)$$

is practically independent of the arrival direction of Cherenkov radiation, i.e., of angles α_i. The same property is exhibited by a structure in which the PMTs are situated at the edges, but this is inconvenient from a technical point of view. In all, five regular polyhedrons are known (the tetrahedron, cube, octahedron, dodecahedron, and icosahedron), and only the first of them does not possess the property of quasisphericity.

Thus, the following main combinations of the photomultipliers forming quasispherical modules are possible: 6, 8, 12, 14, 20, and 32. The property of quasisphericity is most simply explained using the example of the QSM-6 device consisting of six PMTs oriented along the axes of the orthogonal coordinate system (or along the edges of a cube). In general, Cherenkov radiation is registered by three PMTs

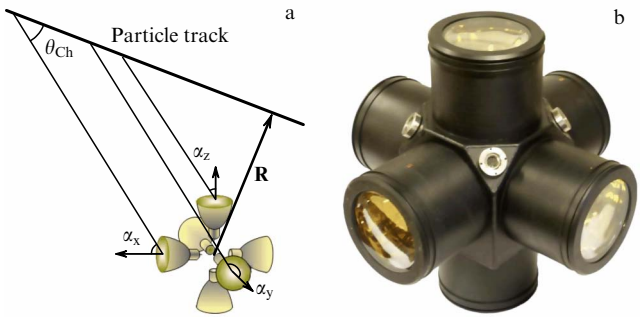

Figure 1. Quasispherical measuring module: (a) registration principle, and (b) external view; θ_{Ch} — Cherenkov angle.

(Fig. 1a) and, if the amplitudes squared of the registered signals are summed up, their sum (or its square root) will not depend on the direction of the Cherenkov radiation, since $(\cos^2\alpha_x + \cos^2\alpha_y + \cos^2\alpha_z)^{1/2} = 1$. Generally, the total response of the quasispherical module, consisting of n identical photomultipliers, is proportional to $(n/6)^{1/2}$.

The first quasispherical module QSM-6 for Cherenkov water detectors was commissioned in 1979 [13]. The structure designed for the CWD ANTARES [14], in which three photomultipliers were directed toward the lower hemisphere at an angle of 75° to each other, served as a certain approximation to a quasispherical module. On the basis of the experience accumulated, the QSM-32 module was developed for a project on a larger scale — a water volume of 1 km^3 (KM3) — in which one of the PMTs was absent, since the connecting cable was input in its place [15]. The creation of CWDs on the basis of such modules provides practically a complete 4π-geometry and identical conditions for the registration of particles arriving from any direction.

4. NEVOD neutrino water detector

The developed QSM-6 quasispherical modules (Fig. 1b) served as the basis for creating the world's first multipurpose CWD of mass 2 kt on Earth's surface with a water reservoir $26 \times 9 \times 9$ m^3 in dimension [10] for resolving, in particular, the ambitious problem of demonstrating the possibility of registering neutrinos on Earth's surface in conditions of a very high background of atmospheric muons (2×10^{10}).

In 1994, the first part of the CWD NEVOD consisting of 25 strings (three or four QSMs in each one) (Fig. 2) and possessing an internal fiducial volume close in shape to a cube with dimensions of $6 \times 6 \times 7.5$ m^3 was commissioned. To calibrate the photomultipliers during prolonged operation, use was made of a system of calibration telescopes (SCT), consisting of 80 scintillation counters, half of which were arranged on the lid of the water basin, while the other half were arranged on its bottom (see Fig. 2). Counters with dimensions of $40 \times 20 \times 2$ cm^3 placed inside waterproof cases and arranged in staggered rows provided for the identification of 1600 different muon trajectories inside the CWD water volume.

The response of QSM to the Cherenkov radiation of muons with known tracks was used for estimation of the rejection coefficient of individual QSM. For this purpose, the SCT was exploited to measure the probability of correct (p) and erroneous (q) determinations of the arrival direction of Cherenkov radiation, and of the absence of information on

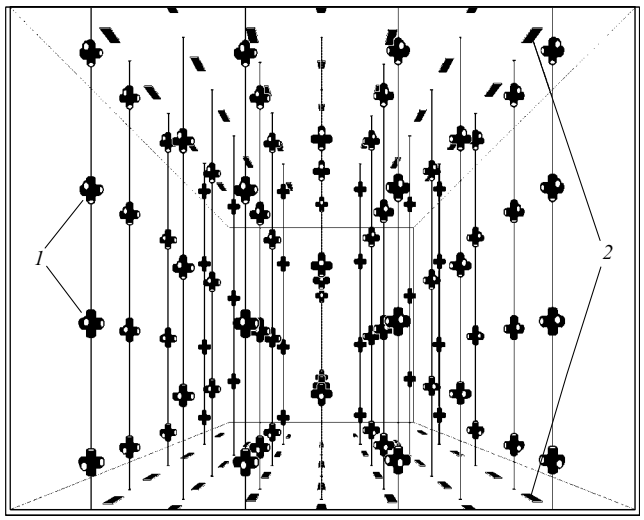

Figure 2. Spatial lattice of a Cherenkov water detector NEVOD: *1* — quasispherical modules, and *2* — scintillation counters of the system of calibration telescopes.

such direction (r) [16]. These quantities are related by the equation: $p + q + r = 1$. The measured distributions of parameters p and q gave the following values for the mean values: $\langle p \rangle = 0.83$, and $\langle q \rangle = 0.023$. The rejection coefficient, which is determined by the ratio p/q, amounts to about 20 per QSM on the average. To single out neutrino events, the value of the rejection coefficient must be 2×10^{10}. Consequently, the minimum excess Δ of the number of modules indicating the correct direction over the number of modules indicating the wrong direction is determined by the relationship $20^{\Delta} > 2 \times 10^{10}$, or $\Delta > 8$.

Figure 3a illustrates an example of the registration of a muon arriving from the upper hemisphere, for which the number of modules indicating the correct direction (from above) is $N_u = 8$, and indicating the wrong direction (from below) is $N_d = 0$; in Fig. 3b, an example is presented of the registration of a muon produced by a neutrino from the lower hemisphere — in this case, the situation is reversed: $N_u = 0$ and $N_d = 8$ [17].

In only four months of running the experiment, two reliably identified neutrino events were registered, together with two candidates for neutrino events [18]. The number of muons due to neutrinos, expected for this period, amounted to 2.5 ± 0.5.

5. Calorimetric properties of a Cherenkov water detector

An important advantage of CWDs over many other charged particle detectors is its calorimetric properties. Usually, a calorimeter represents a heterogeneous structure of detecting elements separated by layers of matter. Here, the energy measurement interval and precision are determined by the number of layers and their thicknesses. The situation in the case of Cherenkov calorimeters is different. The intensity of the Cherenkov radiation increases with the energy of the registered cascade, and more and more distant photomultipliers (or modules composed of them) are fired. The respective distances to the axis of the cascade registered can vary within broad limits, which, in turn, leads to enhancement of the number of measured points in the cascade curve.

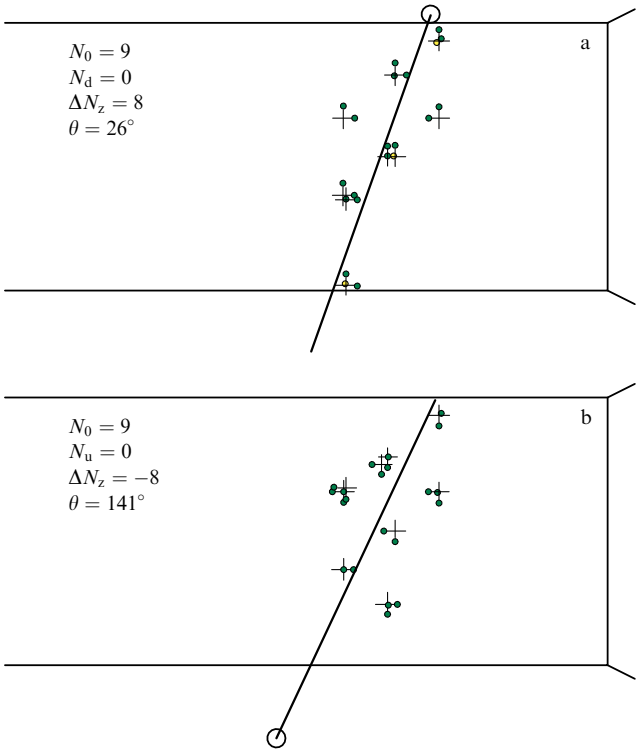

Figure 3. Samples of two 'mirror' events with the same total number of fired modules, N_0, and the same absolute value of the difference $\Delta N_z = N_u - N_d$ (the reconstructed muon tracks are close in angles and of opposite directions): (a) muon from upper hemisphere, and (b) muon from lower hemisphere (due to neutrino).

An investigation of cascade showers generated by cosmic-ray muons in the CWD NEVOD was performed under two selection conditions. In the first case, the cascades studied had axes with known directions that corresponded with good precision to the muon tracks determined by independent detectors. In the second case, the cascade showers were identified by the total energy deposit in the CWD.

In the first case, the problem reduced to determining two parameters of the theoretical cascade curve: the cascade energy ε, and its position on the muon track, which could be chosen to be the cascade starting point, its maximum, or its center of gravity. If the cascade starting point t_0 is used as a parameter, the cascade curve can be approximated as follows [19]:

$$N(\varepsilon, t) = \frac{0.32}{\sqrt{y}} \exp\left[(t - t_0)(1 - 1.5 \ln s)\right], \qquad (3)$$

where $y = \ln(\varepsilon/\beta)$, $\beta = 78.3$ MeV is the critical energy of electrons in water, and $s = 3(t - t_0)/(t - t_0 + 2y)$ is the age of the shower.

The cascade curves were obtained making use of showers generated by muons of the near-horizontal cosmic ray flux propagating along the water detector. For 7945 hours, 1.7 million muons were registered that generated 123,364 cascades of energy higher than 1 GeV. All the cascades were divided into six groups along their logarithmic energy scale with the following mean logarithmic values: 3.16, 10, 31.6, 100, 316, and 1000 GeV.

Figure 4a presents the cascade curves obtained for these energies [20]. Of interest here is the left panel of the figure, where an underlayer is clearly seen that is formed by low-energy cascades, the generation probability of which increases with the muon energy.

In the second case, events are selected by the total energy deposit in the CWD and, when the cascade axis is unknown, the problem becomes significantly more complicated for two reasons: first, a large energy deposit can be caused not only by cascades generated by muons, but also by cascades due to the hadron and electron–photon cosmic ray components and by extensive air showers; second, in reconstructing the cascade curve, four more unknown parameters characterizing the position of the cascade axis appear: two additional coordinates, and two angles. At the same time, the number of such cascades is about two orders of magnitude greater than the number of cascades with a known axis.

In Fig. 4b, energy spectra are presented of cascade showers obtained using the two methods of selection [21]. The interest in investigations of the muon energy spectrum in the energy region above 10 TeV was arisen by the registration in two experiments [22, 23] of an excess of ultrahigh-energy muons, which is one of the sides of the so-called muon puzzle [24].

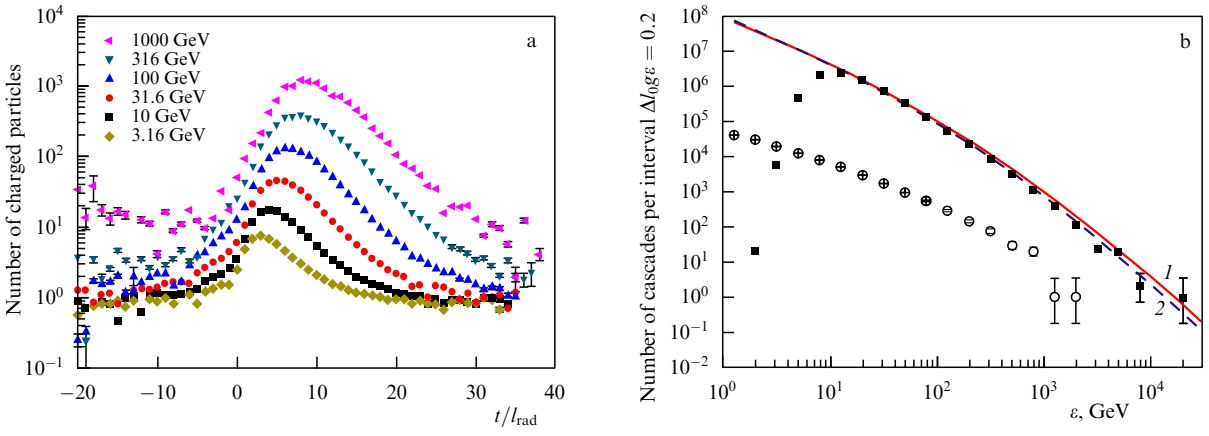

Figure 4. Experimental data for cascades registered by the CWD NEVOD. (a) Average cascade curves of showers with energies within 3.2 – 1000 GeV, and l_{rad} is the radiation length. (b) Spectra of cascade showers produced in water by muons; the squares ($\theta = 50° - 90°$) and circles ($\theta = 85° - 90°$) are experimental data; curves *1* and *2* are calculated results for the integral power spectrum of the generation of parent pions and kaons in the atmosphere with indices $\gamma = 1.7$ and $\gamma = 1.8$, respectively.

6. NEVOD-DECOR complex

The CWD NEVOD exhibits good calorimetric properties, but a low angular precision in measuring particle propagation directions. This is due to its small dimensions, comparable to QSM dimensions (≈ 0.5 m). Therefore, the accuracy of angular measurements amounts to $5^\circ - 7^\circ$, which is acceptable in studies of the vertical flux ($0^\circ - 30^\circ$), when the flux varies insignificantly with the zenith angle, but is absolutely insufficient for studies of muons at large zenith angles ($60^\circ - 90^\circ$), when the flux depends strongly on the zenith angle.

To improve the angular resolution and to provide the possibility of registering multiparticle events, the water basin was surrounded, within the framework of the Russian–Italian project, by a DECOR coordinate detector [25] composed of streamer tube chambers developed for the NUSEX installation [6]. The tubes of dimensions $9 \times 9 \times 3500$ mm^3, the cathodes of which had a resistive coating, while the anode was a 100-micrometer wire, were flushed during operation with a gas mixture composed of argon (25%), carbon dioxide (50%), and n-pentane vapors (25%). The streamer tube chambers were mounted in the modules (in the planes), situated vertically in the galleries surrounding the water detector.

The signal readout from streamers was implemented with the aid of external strips ≈ 1 cm in width, which allowed obtaining two-coordinate information from each plane. Eight such planes 8.4 m^2 in area form a supermodule, which makes it possible to obtain up to eight points in each projection of a particle track and to retrieve its propagation direction with the accuracies of 0.7° and 0.8° for projections of the zenith and azimuthal angles, respectively. Four such supermodules are placed along the lateral (long) side of the basin, and two on the end sides (Fig. 5).

Figure 5 also presents an example of the registration of a single muon by the supermodules situated at opposite end sides of the CWD NEVOD. Such events, termed one-track, are used for calibrating the photomultipliers of the QSM, in particular, those directed downward, since they cannot be calibrated with the aid of the SCT counters.

Still, it is the registration of multimuon events (bundles of muons) at large zenith angles (Fig. 6) that raises greatest interest. From the figure, it is well seen that DECOR only registers part of the particles traversing the Cherenkov water detector. However, taking into account that the dimensions of the detector are much smaller than those of an inclined EAS, the density of muons within the bounds of the installation can be considered constant; this is confirmed by comparing the numbers of muons registered in different supermodules.

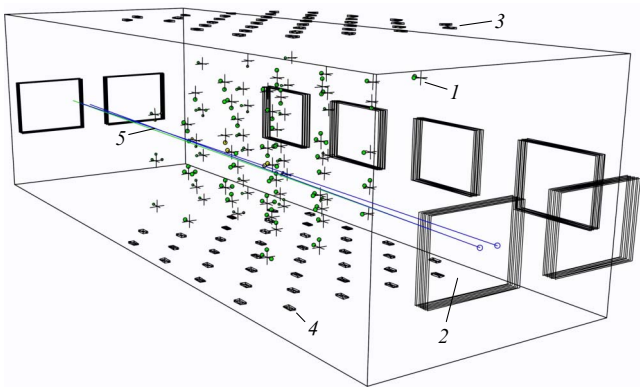

Figure 5. NEVOD-DECOR complex: *1* — quasispherical modules, *2* — supermodules of a coordinate detector, *3* and *4* — counters of upper and lower SCT planes, and *5* — example of a one-track event.

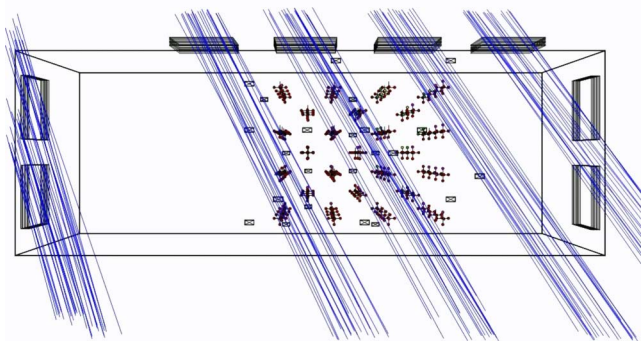

Figure 6. Example of experimental event with a group of muons in the NEVOD-DECOR complex (geometrical reconstruction, view from above).

7. Method of local muon density spectra

Changes in the development of extensive air showers, arriving at different zenith angles, can be traced applying the CORSIKA (COsmic Ray SImulations for KAscade) computer code [26], which permits calculating the characteristics of various EAS components. In Fig. 7a, the results are presented of a simulation of the effective area occupied by the muon component for different zenith angles. Two circumstances draw one's attention: the strong influence of Earth's magnetic field, which essentially increases the EAS size, and the large EAS area at an angle of 85°, which amounts to 6 km^2. In such a situation, a detector of characteristic dimensions of ≈ 100 m^2 can indeed be considered as pointlike, neglecting possible variations in the muon density within its bounds. In this case, it is possible to introduce the concept of local muon density D:

$$D = \frac{m}{S}\,, \tag{4}$$

where m is the multiplicity of muons registered in a given event, and S is the effective area of the detector seen from the muon arrival angle. Then, the spectrum of local muon density for a certain direction can be represented in the form [27]

$$F(\geqslant D) = \int N\big(\geqslant E(\mathbf{r}, D)\big)\,\mathrm{d}S\,, \tag{5}$$

where $\mathbf{r}$ is a point in the cross section of the shower with respect to the EAS axis, and $N(\geqslant E)$ is the integral energy spectrum of primary particles of minimum energy E at which the muon density equals D. This energy is found from the equation

$$\rho(E, \mathbf{r}) = D\,, \tag{6}$$

where $\rho(E, \mathbf{r})$ is a muon lateral distribution function (the density of particles at point $\mathbf{r}$).

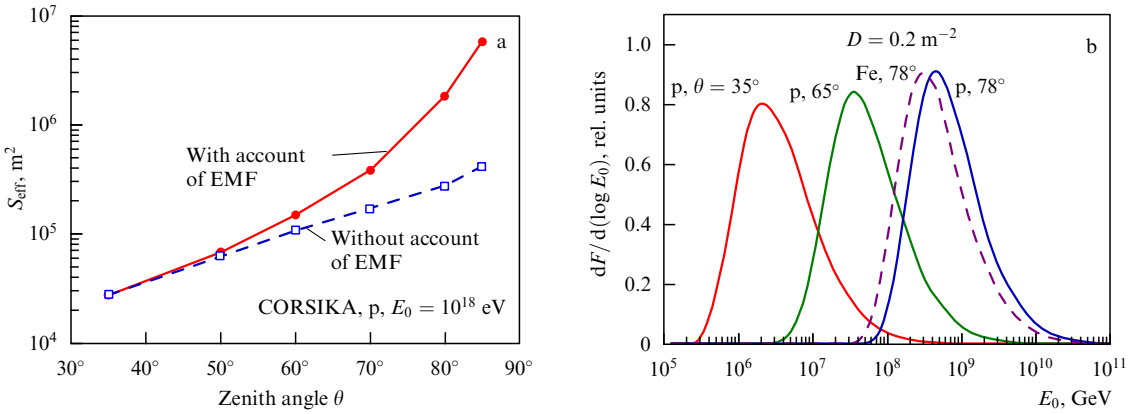

Figure 7. Simulation results. (a) Effective area S_{eff} for collection of muon bundles using the LMDS method; EMF — Earth's magnetic field. (b) Energy distribution of primary particles contributing to events with a fixed muon density. Solid curves — results of calculations for protons (p), and dashed curve — results of calculations for iron nuclei. Values of the zenith angle θ are indicated alongside the curves.

If it is assumed that

$$\rho(E,\mathbf{r}) = \left(\frac{E}{E_0}\right)^{\kappa} \rho(E_0,\mathbf{r})\,, \tag{7}$$

where $\kappa \approx 0.9$, then for the power spectrum of primary particles with an integral index γ, namely

$$N(\geqslant E) = N_0 \left(\frac{E}{E_0}\right)^{-\gamma}, \tag{8}$$

it is possible to obtain from formulas (5)–(8) the following approximate expression for the integral local muon density spectrum (LMDS):

$$F(\geqslant D) = \left(\frac{D}{D_0}\right)^{-\beta} \int \left(\frac{\rho(E_0,\mathbf{r})}{D_0}\right)^{\beta} \mathrm{d}S\,, \tag{9}$$

where $\beta = \gamma/\kappa$, and D_0 is a certain normalizing value of the muon density [in formula (9) it cancels out].

Relationships (6)–(9) permit obtaining estimates of the contributions from different primary energies to the events selected by the muon density at different angles.

In Fig. 7b, clearly seen is the change in energy intervals corresponding to a fixed muon density ($D = 0.2$ m^{-2}) for different zenith angles, which covers three orders of magnitude in energy.

8. Muon puzzle and ways to solve it

An experiment at the NEVOD-DECOR complex was carried out in 2002–2007. In 19,922 hours, over 40 thousand events were collected with muon multiplicities $\geqslant 3$. The results of experimental data processing within the framework of the LMDS method and their comparison with the results of simulation are presented in Fig. 8 for four values of the zenith angle [27].

From Fig. 8a, the experimental data in the energy region of $10^{15} - 10^{16}$ eV (zenith angle 35°) are seen to correspond to the normal composition of cosmic rays. A sharp bend is clearly watched in the energy spectrum in the middle of this interval (the so-called knee), which confirms that absolute referencing by the LMDS method is performed correctly. As the zenith angle increases (Fig. 8b, $\theta = 50°$), the experimental points are seen to approach the calculated results for cosmic rays composed of iron nuclei. At an energy of $\sim 10^{17}$ eV (Fig. 8c), a second bend is observed in the energy spectrum (the second knee), while the cosmic ray mass composition corresponds to pure iron. As the energy further increases (Fig. 8d), the experimental data go beyond the bounds of possible estimates of the muon flux in EASs applying existing models for a purely iron composition of the primary cosmic rays. This result was confirmed in experiments carried out at CERN with the ALEPH (Apparatus for Large Electron Positron collider pHysics) [28], DELPHI (DEtector with Lepton, Photon and Hadron Identification) [29], and L3-C [30] installations, and at the world's largest array of detectors for EAS investigations in the Pierre Auger Observatory in Argentina [31].

The problem of the excess of muons in EASs, which increases with their energy together with the aforementioned excess of ultrahigh-energy (> 100 TeV) muons in their inclusive spectrum [22, 23], was termed the 'muon puzzle' [24]. The reasons for such a behavior of the muon component can be both of cosmophysical character (a strong change in the cosmic ray spectrum and of their composition, including a change due to particles heavier than the iron nucleus) and of a nuclear-physical character (a change in the hadron interaction producing heavy particles or states of matter). The second version is supported by other anomalies registered in cosmic rays: halos, alignment, penetrating cascades, Centaurs (anti-Centaurs), events with large transverse momenta, and so on, which cannot be described within the framework of existing models of hadron interactions [32, 33].

To explain all the anomalies observed in cosmic rays, a model for the production in nucleus–nucleus interactions of a quark–gluon matter (QGM) blob with a high orbital momentum was put forward in papers [34, 35]. The effective mass of this blob is ~ 1 TeV, while its orbital momentum L can amount to values of $10^3 - 10^4$ [36]. In this case, such a blob can be considered a resonance with a high centrifugal barrier

$$V(L) \sim \frac{L^2}{2mR^2}\,, \tag{10}$$

where m is the mass of the QGM blob, and R is its size.

In the case of light quarks, the height of the barrier will be quite large and the respective decays will be strongly suppressed. At the same time, the centrifugal barrier for top-quarks turns out to be small, and the probability of their being

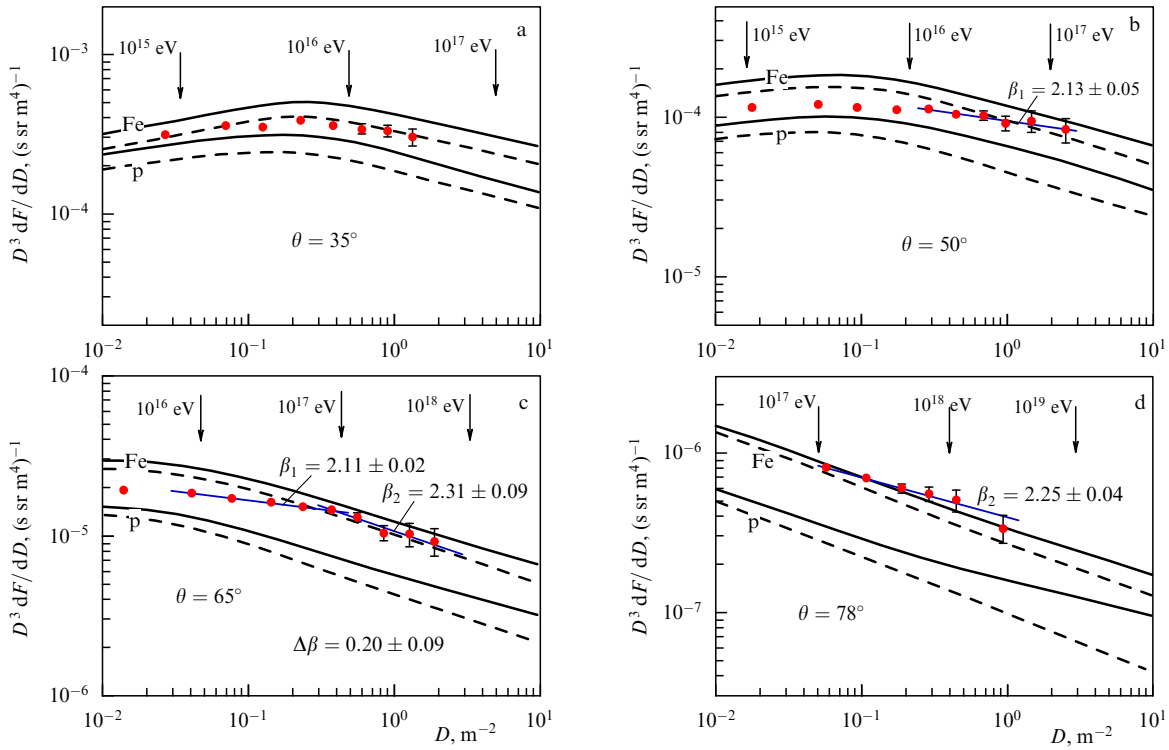

Figure 8. Experimental and calculated differential spectra of local muon density for zenith angles 35° (a), 50° (b), 65° (c), and 78° (d). Circles — experimental data, solid curves — results of calculations by QGSJET01 model (Quark Gluon String model with JETs), and dashed curves — calculations by SIBYLL model. The lower pairs of curves in figures a–d correspond to primary protons, and the upper pairs to iron nuclei.

produced and escaping increases significantly. This essentially changes the character of hadron interactions and permits an explanation of all the anomalous phenomena registered in cosmic rays, including the muon puzzle.

The experimental possibility of resolving the muon puzzle is related to measurements of the energy deposit of the EAS muon component, which is the only parameter that has not been investigated yet. In the case of the cosmophysical nature of the muon excess origination, their specific energy deposit per muon will depend weakly on the energy of the primary particles. In the nuclear-physical version, the dependence of the specific energy deposit should change owing to the increasing contribution from high-energy muons.

9. Energy deposit of muon bundles in the Cherenkov water detector NEVOD

An experiment on measuring the energy deposit of muon bundles was started at the NEVOD-DECOR complex in 2012. The DECOR coordinate detector was exploited to determine the number of muons in a bundle, while with the aid of a Cherenkov water detector measurements were made of the energy deposit within its fiducial volume. Processing the experimental results obtained in 9,673 hours of registration yielded the following results [37]. Within the $55° - 90°$ interval of zenith angles, 16,416 events were registered, involving the number of muons $\geqslant 5$. To investigate the energy deposit behavior at small angles, events were processed that were registered within the $40° - 55°$ interval of zenith angles. In 3253 hours, 15,084 events were registered. The specific energy deposit was estimated with account of the registered particle multiplicity and the angles at which the particles traversed the CWDs.

Figure 9a presents the zenith angle dependence of the specific energy deposit (in photoelectrons). Two regions of zenith angles are well identified: below $\approx 55°$, and above $\approx 55°$. The first interval corresponds to absorption of the hadron and electron–photon EAS components with an absorption length $\Lambda = 134 \pm 15$ g cm^{-2}. The second interval corresponds to the energy deposit of the pure muon component. Enhancement of this energy deposit can be traced to being related to an increase in the mean muon energy in the bundles, when they are registered at large zenith angles, which corresponds to the results of calculations by the CORSIKA program [26]. To estimate possible systematic distortions, the dependence was constructed of the energy deposit on the azimuthal angle. The dependence obtained revealed no anomalies and, within the limits of statistical errors, it can be described by a constant.

The dependence of the specific energy deposit on the multiplicity of registered muons (Fig. 9b) is apparently more interesting. Although the database statistics obtained are not large, the enhancement outlined in the specific energy deposit at energies of primary particles over $\sim 10^{17}$ eV may testify in favor of the existence of a certain new source generating high- and ultrahigh-energy muons. Further enhancement of collected statistics, as well as the resolution of certain methodical issues related to measurements of muon densities and of their energy deposit in the CWD NEVOD, will permit us to draw more reliable conclusions.

In discussing ways to resolve the muon puzzle within the framework of the nuclear-physical approach, the question inevitably arises concerning the possibility of searching for new particles (states of matter) responsible for its origination in experiments at the Large Hadron Collider (LHC) [38]. Indeed, the region of energies close to $\sim 10^{16}$ eV, in which the

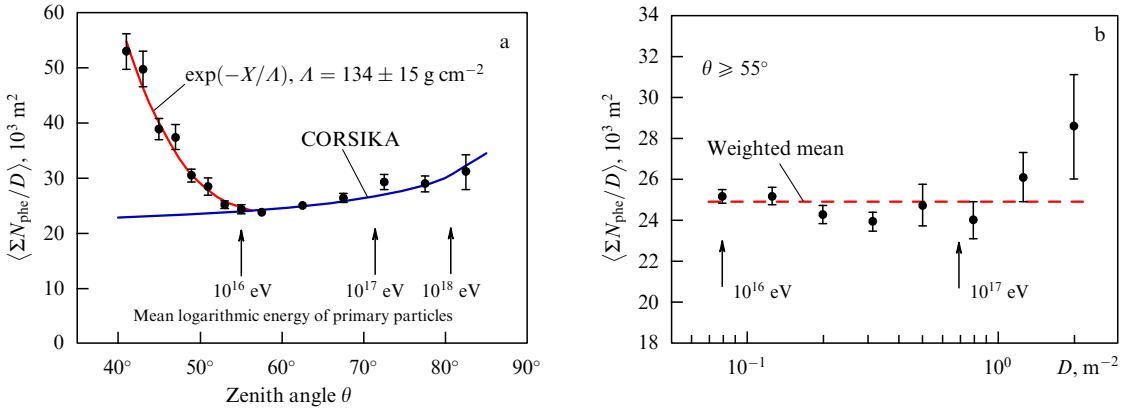

Figure 9. Dependence of the specific energy deposit of muon bundles on (a) the zenith angle θ, and (b) the muon density D in the bundles.

threshold for the onset of new physics is apparently to be found, corresponds to the LHC range of energies. In cosmic rays, however, this energy interval corresponds to nucleus–nucleus interactions, while in experiments at LHC, it corresponds to proton–proton interactions for which the formation threshold of quark–gluon matter blobs will be significantly higher. As to nucleus–nucleus interactions, searches for the top quarks in such interactions are rendered quite difficult, owing to the large multiplicities of secondary particles. Therefore, in the coming years the NEVOD-DECOR complex will remain the only installation in the world at which such studies can be implemented, since at other installations no possibility exists of measuring the muon component energy deposit necessary for the investigation of EASs.

10. Further prospects

Although the NEVOD-DECOR experiment, the scope of which is to measure the energy deposit of the muon component of inclined EASs, is unique, it does exhibit certain drawbacks. First, the supermodules of DECOR do not fully cover the Cherenkov water detector (see Fig. 6), and this leaves some uncertainty in the estimation of muon multiplicity. And, while the concept of the LMDS method is based on the weakly changing spatial distribution of muons within scales of installations such as DECOR, quite large fluctuations are possible in the number of muons registered, especially in the case of small multiplicities.

Second, the water reservoir is only partially filled with measurement modules, which results in muon bundles traversing the CWD at different points, giving rise to different responses. Furthermore, although this circumstance can be taken into account by calculations, the spread in responses to individual events may turn out to be quite significant.

Third, the position of the EAS axis with respect to the NEVOD-DECOR experimental complex being unknown results in a large spread in estimates of primary particle energies, which are responsible for the formation of muon bundles with certain multiplicities and zenith angles (Fig. 7b).

At present, a development program of the unique scientific facility NEVOD Experimental Complex (EC) has been prepared, within the framework of which further expansion is planned of the CWD, as well as the construction of new detectors. A new external coordinate-tracking detector, TREK, will be created on the basis of drift chambers previously exploited in the neutrino detector at the U-70 accelerator of the Institute for High Energy Physics (IHEP) in Protvino. This work is performed within the framework of a collaboration between the National Research Nuclear University MEPHI and IHEP [39]. The area of the new installation will amount to 260 m^2 and will cover the whole lateral side of the CWD. Here, the precision in separating muon tracks will be improved from 3 cm in the existing detector to 0.3 cm in the new detector, which will permit obtaining more reliable data on muon multiplicities in the region of ultrahigh energies.

The upgrade of the Cherenkov water detector will be realized by expanding its detecting system over the entire volume of the water reservoir. This will eliminate the problem concerning the dependence of the CWD response to the positions of particle trajectories. At the same time, such a CWD can be applied in studies of the energy spectrum of the near-horizontal cosmic ray flux by the pair meter method (by measuring cascades generated as a result of electron–positron pair production).

An array for registering the EAS electron–photon component of cosmic rays is to be accommodated around the NEVOD EC building [40]. To this end, scintillation detectors will be utilized that were previously applied in the installations EAS-TOP [Extensive Air Showers (EAS) on TOP of Gran Sasso underground laboratories] [41] and KASCADE-Grande (KArlsruhe Shower Core and Array DEtector-Grande) [42]. In accordance with the Agreement between MEPHI and the National Institute for Nuclear Physics (INFN, Italy), these detectors will be used in the NEVOD-EAS installation [40].

Construction is also planned of an installation for registering atmospheric neutrons (URAN), which will become the first large-scale installation in the world for investigating the EAS neutron component [43].

Upon implementation of the above development program, the NEVOD experimental complex will become a scientific installation of a mega-science class and will permit the investigation of practically all the cosmic ray components within the record wide energy interval from 10^9 to 10^{19} eV (Fig. 10) and within the complete range of zenith and azimuthal angles.

11. Conclusion

Creation of the Cherenkov water detector NEVOD opened a new field for the research of different cosmic ray components

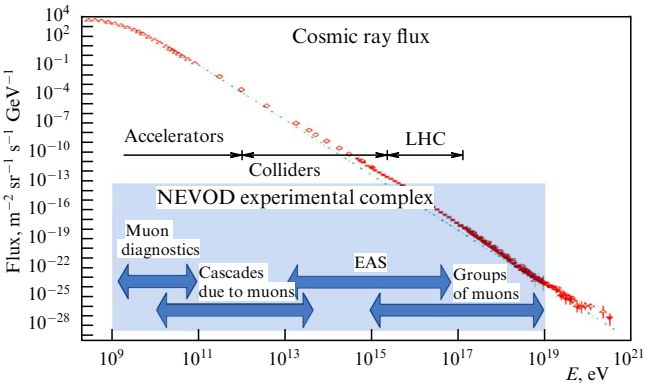

Figure 10. Energy intervals for different methods used in the NEVOD experimental complex for registration of cosmic rays.

on Earth's surface. Unlike underground (under-ice) detectors, NEVOD effectively registers inclined showers and near-horizontal muon fluxes. The characteristic features of Earth's atmosphere present unique possibilities for registering bundles of muons from primary particles with energies up to 10^{19} eV exploiting an installation of relatively small dimensions, and they also enhance the flux of high-energy muons near the horizon, which can be registered applying both the calorimetric method and the pair meter method.

The experimental complex created on the basis of the CWD NEVOD and undergoing constant development was included on the list of unique scientific installations of the Russian Federation. After realization of the Development Program in 2015–2020, the NEVOD experimental complex will become an installation of a mega-science class for performing fundamental, search, and applied studies of cosmic rays with record wide energy interval — 10^9–10^{19} eV — within the complete range of zenith and azimuthal angles.

The present article was written on the basis of results obtained at the unique NEVOD facility with the support of the Russian Federation Ministry of Education and Science (project RFMEF159114X0002 and state assignment) and the Russian Federation President's Grant NSh-4930.2014.2.

References

1. Fukuda S et al. *Nucl. Instrum. Meth. Phys. Res. A* **501** 418 (2003)
2. Balkanov V A et al. (Baikal Collab.), in *Proc. of the 25th Intern. Cosmic Ray Conf., Durban, South Africa, 30 July – 6 August, 1997* Vol. 7 (Durban, 1997) p. 21
3. Ageron M et al. *Nucl. Instrum. Meth. Phys. Res. A* **656** 11 (2011)
4. Achterberg A et al. (IceCube Collab.) *Astropart. Phys.* **26** 155 (2006)
5. Roberts A, Wilkins G A (Eds) *Proc. of the 1978 DUMAND Summer Workshop, La Jolla, Calif., July 24 – September 2, 1978* (La Jolla, Calif.: DUMAND, Scripps Institution of Oceanography, 1979)
6. Battistoni G et al. *Nucl. Instrum. Meth. Phys. Res. A* **245** 277 (1986)
7. Berger Ch et al. (Fréjus Collab.) *Nucl. Instrum. Meth. Phys. Res. A* **262** 463 (1987)
8. Nakamura K et al., in *Physics and Astrophysics of Neutrinos* (Eds M Fukugita, A Suzuki) (Tokyo: Springer-Verlag, 1994) p. 249
9. Becker-Szendy R et al. *Nucl. Instrum. Meth. Phys. Res. A* **324** 363 (1993)
10. Abin A V et al., in *21st Intern. Cosmic Ray Conf., Adelaide, Australia, 1990, Conf. Papers* Vol. 10 (Ed. R J Protheroe) (Northfield: Department of Phys. and Math. Phys., The Univ. of Adelaide, Graphic Services, 1990) p. 234
11. Atkins R et al. (The Milagro Collab.), astro-ph/0110513
12. Bobisut F et al., in *3rd Intern. Workshop on Neutrino Telescopes, Venezia, Italy, February 26 – 28, 1991* (Ed. M Baldo Ceolin) (Venice, 1991) p. 387
13. Borog V V et al., in *16th Intern. Cosmic Ray Conf., Kyoto, 1979* Vol. 10 (Ed. S Miyake) (Tokyo: Institute for Cosmic Ray Research, Univ. of Tokyo, 1979) p. 380
14. Amram P et al. (The ANTARES Collab.) *Nucl. Instrum. Meth. Phys. Res. A* **484** 369 (2002)
15. Adrián-Martínez S et al. *Eur. Phys. J. C* **74** 3056 (2014)
16. Aynutdinov V M et al., in *6th Intern. Workshop on Neutrino Telescopes, Venezia, Italy, 1994* (Ed. M Baldo Ceolin) (Venice, 1994) p. 565
17. Aynutdinov V M et al. *Nucl. Phys. B Proc. Suppl.* **70** 489 (1999)
18. Aynutdinov V M et al. *Nucl. Phys. B Proc. Suppl.* **66** 235 (1998)
19. Greisen K, in *Progress in Cosmic Ray Physics* Vol. 3 (Ed. J G Wilson) (Amsterdam: North-Holland, 1956) p. 1
20. Khokhlov S S et al. *Bull. Lebedev Phys. Inst.* **41** 292 (2014); *Kratk. Soobshch. Fiz. FIAN* **41** (10) 31 (2014)
21. Khomyakov V A et al. *Bull. Russ. Acad. Sci. Phys.* **79** 371 (2015); *Izv. Ross. Akad. Nauk Fiz.* **79** 405 (2015);
22. Bogdanov A G et al. *Astropart. Phys.* **36** 224 (2012)
23. Berghaus P, Xu C "Atmospheric muon spectrum from catastrophic energy losses in IceCube", in *32nd Intern. Cosmic Ray Conf., August 11 – 18, 2011, Beijing, China*
24. Petrukhin A A *Nucl. Instrum. Meth. Phys. Res. A* **742** 228 (2014)
25. Barbashina N S et al. *Instrum. Exp. Tech.* **43** 743 (2000); *Prib. Tekh. Eksp.* (6) 20 (2000)
26. Heck D et al., Report FZKA 6019 (Karlsruhe: Forschungszentrum Karlsruhe GmbH, 1998)
27. Bogdanov A G et al. *Phys. Atom. Nucl.* **73** 1852 (2010); *Yad. Fiz.* **73** 1904 (2010)
28. Avati V et al. *Astropart. Phys.* **19** 513 (2003)
29. Abdallah J et al. (Delphi Collab.) *Astropart. Phys.* **28** 273 (2007)
30. Wilkens H, L3 Collab., in *Proc. of the 28th Intern. Cosmic Ray Conf., July 31 – August 7, 2003, Tsukuba, Japan* Vol. 3 (Eds T Kajita et al.) (Tokyo: Universal Acad. Press, 2003) p. 1131
31. Rodriguez G (for the Pierre Auger Collab.) *EPJ Web Conf.* **53** 07003 (2013)
32. Petrukhin A A, in *Vulcano Workshop Frontier Objects in Astrophysics and Particle Physics 2004* (Eds F Giovannelli, G Mannocchi) (Bologna, 2005) p. 489
33. Petrukhin A A *Nucl. Phys. B Proc. Suppl.* **151** 61 (2006)
34. Petrukhin A, in *Frontier Objects in Astrophysics and Particle Physics, Vulcano Workshop 2006, 22 – 27 May 2006, Vulcano, Italy* (Eds F Giovannelli, G Mannocchi) (Bologna, 2007) p. 497
35. Petrukhin A A *Nucl. Phys. B Proc. Suppl.* **175 – 176** 125 (2008)
36. Gao J-H et al. *Phys. Rev. C* **77** 044902 (2008)
37. Kokoulin R P et al. *Bull. Russ. Acad. Sci. Phys.* **79** 365 (2015); *Izv. Ross. Akad. Nauk Fiz.* **79** 398 (2015)
38. Petrukhin A A *Acta Polytechnica* **53** (Suppl.) 707 (2013)
39. Zadeba E A et al. *JINST* **9** C08018 (2014)
40. Shulzhenko I A et el. *Bull. Russ. Acad. Sci. Phys.* **77** 641 (2013); *Izv. Ross. Akad. Nauk Fiz.* **77** 707 (2013)
41. Aglietta M et al. *Nucl. Instrum. Meth. Phys. Res. A* **336** 310 (1993)
42. Apel W D et al. *Nucl. Instrum. Meth. Phys. Res. A* **620** 202 (2010)
43. Gromushkin D M et al. *JINST* **9** C08028 (2014)